

# Spectroscopic Investigations on the H-Type Aggregation of Coumarin 153 Dye Molecules: Role of Au Nanoparticles and $\gamma$ -Cyclodextrin

Tapasi Sen · Santanu Bhattacharyya ·  
Sadananda Mandal · Amitava Patra

Received: 9 June 2011 / Accepted: 30 August 2011 / Published online: 10 September 2011  
© Springer Science+Business Media, LLC 2011

**Abstract** Here, we study the formation of H-type aggregation of coumarin 153 (C153) dye molecule in presence of Au nanoparticles and the removal of dye aggregation in presence of  $\gamma$ -cyclodextrin (CD) due to confinement of dye molecules inside the nanocavity of  $\gamma$ -cyclodextrin (CD) using steady state and time resolved spectroscopy. Blue shifting of absorption band, photoluminescence (PL) band and the enhancement of decay time of C153 dye confirm the formation of H-aggregation. It is found that the concentrations of  $\gamma$ -CD and Au nanoparticles play an important role on H-type aggregation of dye. The rotational relaxation time of free C153 is 0.113 ns and the average relaxation time of C153 dye are 0.275 ns and 0.425 ns for 2 mM and 5 mM  $\gamma$ -CD confined systems, respectively, indicating the anisotropy increases due to confinement of dye. An associated type anisotropy decay of C153 dye is found at 20 mM concentration of CD may be due to formation of nanotubular aggregates of  $\gamma$ -CD.

**Keywords**  $\gamma$ -Cyclodextrin · Coumarin 153 dye · Au nanoparticles · Aggregation · Time-resolved spectroscopy

## Introduction

The interaction of fluorophores with metallic particles is likely to become an active area of research. The most advantage of Au nanoparticles is that these nanoparticles

could be used as acceptors in biophysical experiments in vitro as well as in vivo. Metal nanoparticles based resonance energy transfer has recently gained interest in finding out the potential applications because metal plasmon resonances have revealed unexpected electrodynamic properties [1–8]. Interaction of the electroactive dye molecules with metal nanocluster very often leads to the aggregation effect [9]. These types of hybrid organic–inorganic moieties have promising applications in developing efficient light energy conversion systems, optical and sensor devices [10, 11]. Besides, it has great utility in photoelectrochemical cell as light harvesting antenna materials and as well as photo sensitizer [12–15]. It is demonstrated theoretically that the nature of the molecular orientation of the dye molecules in the aggregated state determines the spectral shift in the absorption band. In case of H-type aggregation, there is blue shift of the absorption spectra due to parallel orientation [16]. Two new excitonic bands are formed, one with higher energy and other with lower than the monomer energy level. Thus, non-radiative energy transfer occurs from higher energy state to lower energy state [16] and aggregated moieties have lower fluorescence property. It is well known that the absorption band red shifted in case of J-type aggregation due to anti parallel orientation. Formation of aggregated species alters the photoluminescence spectra of the dye molecules with respect to monomer. As a result aggregated state show new photosensitizing properties. Kamat et al. [17] has reported the efficient H-aggregation behavior of Rhodamine 6 G on the surface of semiconducting oxide nanoparticles. Kerker et al. [18] has also reported the aggregation of similar dye on the Ag nanoparticles surface [18]. Besides, Ghosh et al. [19] has demonstrated the J-aggregation behavior of eosin dye on Au nanoparticles surface. They also reported the effect of metal nanoparticles size on the aggregation

T. Sen · S. Bhattacharyya · S. Mandal · A. Patra (✉)  
Department of Materials Science,  
Indian Association for the Cultivation of Science,  
Kolkata 700 032, India  
e-mail: msap@iacs.res.in

behavior. On the other hand few groups already have demonstrated the aggregation dependent photophysical properties of various dye molecules on metal surfaces [20–23].

The investigations on chromophores confined in nanocavity have recently opened up new possibilities for light harvesting applications [24–27]. Tunability of the highly organized materials offers fascinating new possibilities for exploring energy transfer phenomena for developing new challenging photonic devices [28]. Among all potential hosts, the cyclodextrin seems to be the most important ones because of several advantages.  $\gamma$ -cyclodextrins (CDs) are cyclic oligosaccharides compounds in which eight glucose units are linked to form a truncated conical structure [29]. The interior cavity of  $\gamma$ -CD is hydrophobic in nature having dimension of 7.5–8.5 Å and the height of ~8 Å [29]. Therefore, large number of organic molecules can be encapsulated in its hydrophobic cavity and form host-guest supramolecular structures. It is also well known that cyclodextrins form nanostructured aggregates through hydrogen bonding. McGown et al. [30–32] reported the formation of rigid molecular nanotube aggregates of  $\beta$ -CD and  $\gamma$ -CD through linkage by the rodlike molecules of DPH. These nanostructures generated much interest as alternatives to the carbon nanotube in the design of supramolecular assemblies to serve as molecular devices. It is also reported the formation of large linear nanotube aggregates of  $\gamma$ -CD linked by coumarin 153 dyes and the temperature effect on rotational dynamics of Coumarin 153 in  $\gamma$ -CD cavity [33]. Recently, the formation of elongated nanotubular aggregates of Au nanoparticle functionalised  $\gamma$ -CD with confined C480 dye have been reported. In this case almost 99% of PL-quenching occurred for C480 in presence of  $\gamma$ -CD attached Au nanoparticles [34].

To the best of our knowledge, there is no detailed spectroscopic study on nature of coumarin 153 dye aggregations in presence of Au nanoparticles and the removal of these dye aggregation using  $\gamma$ -Cyclodextrin nanocavity. This paper focuses on how the concentrations of Au nanoparticles and  $\gamma$ -CD influence on the aggregation of dye molecules.

### Preparation of Citrate Stabilized Gold Nanoparticles

Coumarin 153 (C153) (Sigma-Aldrich),  $\gamma$ -cyclodextrin ( $\gamma$ -CD) (Aldrich), chloroauric acid ( $\text{HAuCl}_4 \cdot 3\text{H}_2\text{O}$ ) (S.d.Fine Chem), Tri-sodium citrate dihydrate (Merck) were used as received. Gold colloids of fairly uniform size were prepared by well-known citrate reduction method reported by Graber et al. [35]. Briefly, 50 ml aqueous solution of  $\text{HAuCl}_4$  (1 mM) was heated to boiling with vigorous stirring. Then 2.5 mL of 50 mM sodium citrate solution was added to the

boiling solution with vigorous stirring. The color of the solution changes from light yellow to deep red within 5–10 mins of heating. Then, the solution was allowed to boil for another 10 min. Stirring was continued until the solution reached to room temperature. The concentration of as prepared gold nanoparticles solution was 12 nM. The size of Au nanoparticle is 14 nm as we reported previously [36].

For the preparation of dye confined in the cavity of cyclodextrin, 1 mL of 10  $\mu\text{M}$  Coumarin 153 dye solution was added to 5 ml of 20 mM  $\gamma$ -CD solution. This solution was kept for 1 day at room temperature for inclusion of dye in the cyclodextrin cavity. After 1 day, as prepared Au solution (0.182 ml) was added to 2 ml of C153  $\gamma$ -CD solution to maintain the concentration of Au 1 nM. We have varied the concentration of  $\gamma$ -CD from 20 mM to 2 mM by only adjusting the amount of  $\gamma$ -CD in aqueous solution. Further, we have changed the Au nanoparticles concentration in stock solution from 4 nM to 0.25 nM for different measurements.

### Characterization

The emission spectra of all samples were recorded in a fluoro Max-P (HORIBA JOBIN YVON) Luminescence Spectrophotometer. For the time correlated single photon counting (TCSPC) measurements, the samples were excited at 405 nm using a picosecond diode laser (IBH Nanoled-07) in an IBH Fluorocube apparatus. The typical fwhm of the system response using a liquid scatter is about 90 ps. The fluorescence decays were collected on a Hamamatsu MCP photomultiplier (C487802). The fluorescence decays were analyzed using IBH DAS6 software. For anisotropy measurements, a polarizer was placed before the sample. The analyzer was rotated by 90° at regular intervals and the parallel ( $I_{\parallel}$ ) and the perpendicular ( $I_{\perp}$ ) components for the fluorescence decay were collected for equal times, alternatively. Then,  $r(t)$  was calculated using the formula [37]

$$r(t) = \frac{I_{\parallel}(t) - GI_{\perp}(t)}{I_{\parallel}(t) + 2GI_{\perp}(t)} \quad (1)$$

The G value of the setup is 0.58.

### Results and Discussion

Figure 1 shows the PL-spectra of Coumarin 153 dye at different concentrations of  $\gamma$ -CD with and without 1 nM Au nanoparticles. The PL band of free C153 dye in water is observed at 545 nm. The PL band gradually blue shifted (from 544 nm to 535 nm) and quantum yield increases with increasing the concentration of  $\gamma$ -CD (Fig. 1b to e). This

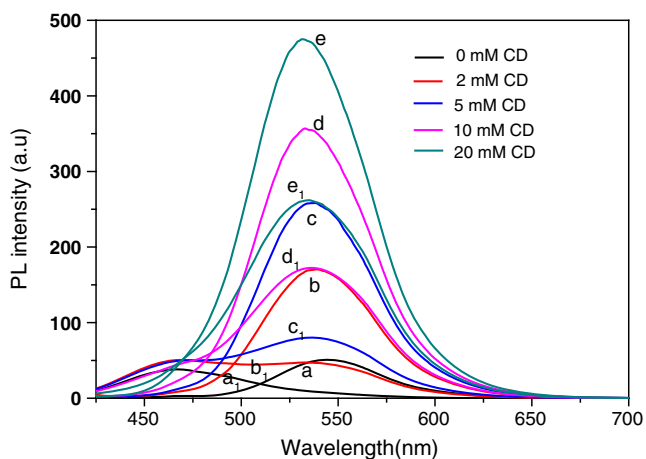


**Fig. 1** PL spectra of C153 confined in (a) 0 mM, (b) 2 mM, (c) 5 mM, (d) 10 mM and (e) 20 mM  $\gamma$ -CD concentration. The corresponding PL spectra in presence of 1 nM Au nanoparticles are showing in subscript 1. ( $\lambda_{ex}$ =405 nm)

results match well with the previous results [37]. It indicates that the confinement effect increases with increasing the  $\gamma$ -CD concentration. It is interesting to note that the PL band of free C153 is shifted from 544 nm (Fig. 1a) to 470 nm (Fig. 1a<sub>1</sub>) in presence of Au nanoparticles. This blue shifting may be due to H-aggregation of dye molecules in presence of Au nanoparticles. It is interesting to note that this blue shifted peak gradually shifted back to its original peak position at about 535 nm with increasing the concentration of CD (Fig. 1b<sub>1</sub> to e<sub>1</sub>). It indicates that the C153 dye molecule is encapsulated in its hydrophobic cavity of  $\gamma$ -CD. In fact, we did not observe any band at 470 nm when the concentration of  $\gamma$ -CD is 20 mM. At higher CD concentration most of the C153 monomers are confined in  $\gamma$ -CD nanochannel to avoid aggregation of dye. However, at lower concentration of  $\gamma$ -CD, a certain fraction of C153 is free in water and these free C153 monomers became aggregated in presence of Au nanoparticles.

To understand the aggregation behavior of C153 dye in presence of Au, we have used 2 mM  $\gamma$ -CD concentration and varying the Au nanoparticles concentration from 0.25 nM to 4 nM. The certain fraction of C153 is found to be free in water at 2 mM  $\gamma$ -CD concentration. Therefore, the interaction with Au nanoparticles should be clearly understood at this  $\gamma$ -CD concentration. Figure 2a depicts the UV-vis spectra of C153 confined in 2 mM CD in presence of different concentrations of Au nanoparticles. The absorption band of pure C153 dye in water is obtained at 430 nm. The absorption spectra of C153 in presence of different concentrations of Au nanoparticles show another

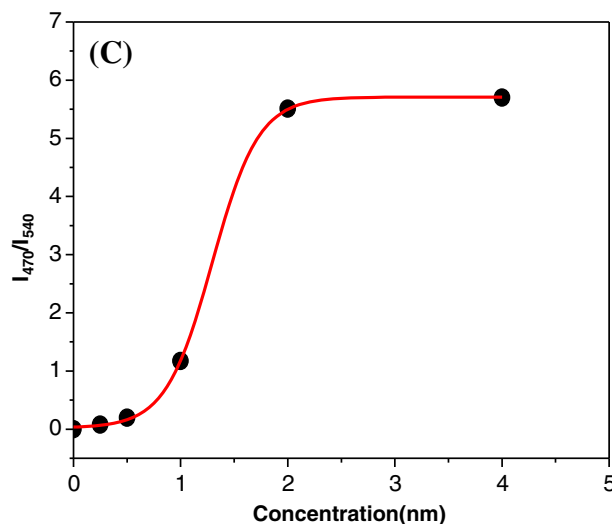
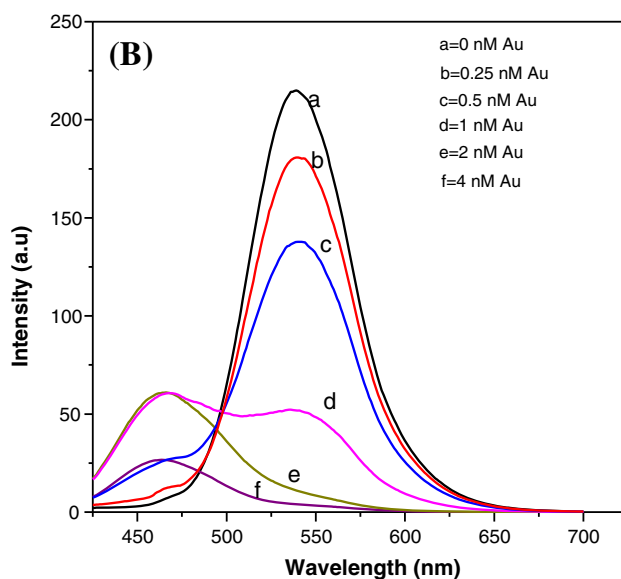
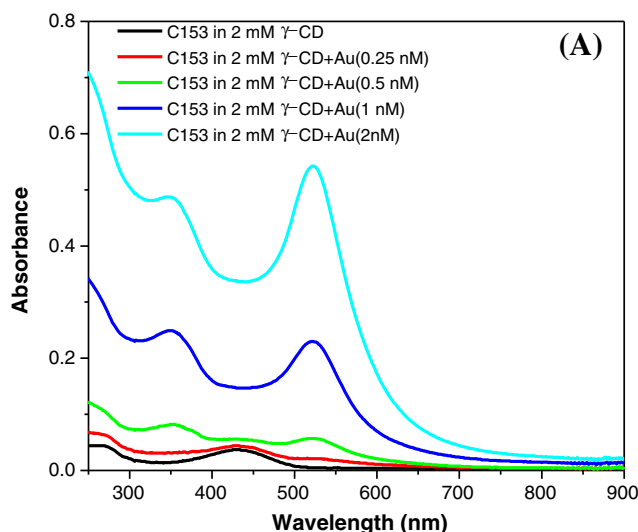


**Fig. 2** a UV-vis absorption spectra and (b) photoluminescence spectra of C153 in presence of different concentrations of Au nanoparticles. c A plot of  $I_{470}/I_{540}$  vs. concentration of Au nanoparticles where the concentration of  $\gamma$ -CD is 2 mM

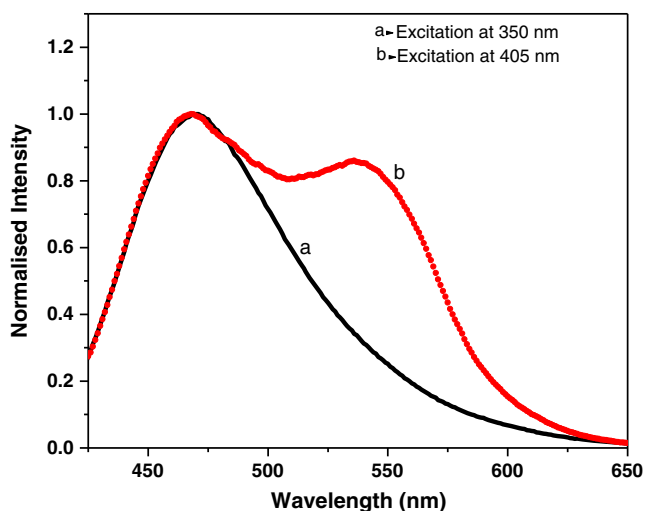


**Fig. 3** PL spectra of C153 confined in 2 mM  $\gamma$ -CD at different excitation wavelengths (Concentration of Au nanoparticles is 1 nM)

band at 520 nm which is the characteristic surface plasmon resonance band of Au nanoparticles. A blue shifted absorption band at 350 nm appears in presence of Au nanoparticles. The intensity of higher energy band at 350 nm increases and the band at 430 nm disappears with increasing the concentration of Au nanoparticles. It may be due to intermolecular H-type of aggregation between C153 monomers in presence of Au nanoparticles. Various works have been done on the aggregation behavior of dye molecules on the metal nanoparticles surface. H-aggregation of rhodamine 6 G on metal nanoparticles surface have been reported previously [17, 18]. As we previously mentioned that the transition to upper excitonic state is only allowed in case of H-aggregation that will show the hypsochromic shift of the absorption spectra [19]. Figure 2b depicts the photoluminescence spectra of C153 confined in 2 mM  $\gamma$ -CD in presence of different concentrations of Au nanoparticles. H-aggregated emission band at 470 nm became relatively prominent with increasing the concentration of Au nanoparticles. A small hump at 470 nm appears in presence of 0.25 nM Au nanoparticles concentration and the intensity of this band increases with increasing the concentration of Au from 0.5 nM to 1 nM. With further increase of Au nanoparticle concentration (4 nM), the peak at 540 nm disappeared. In this particular situation only band at 470 nm is observed. It clearly indicates that higher amount of H-aggregation is obtained at higher concentration of Au nanoparticles. It reveals that Au nanoparticles influence the H-aggregation of C153 molecules. In present system, concentration dependent self aggregation of dye is not possible because the concentration of C153 is in micromolar region. Therefore, the affecting factor is the interaction of dye molecules with Au nanoparticles. Figure 2c shows the plot of  $I_{470}/I_{540}$  vs. concen-

tration of Au nanoparticles. With increasing concentration of Au the value of  $I_{470}/I_{540}$  increases and it became

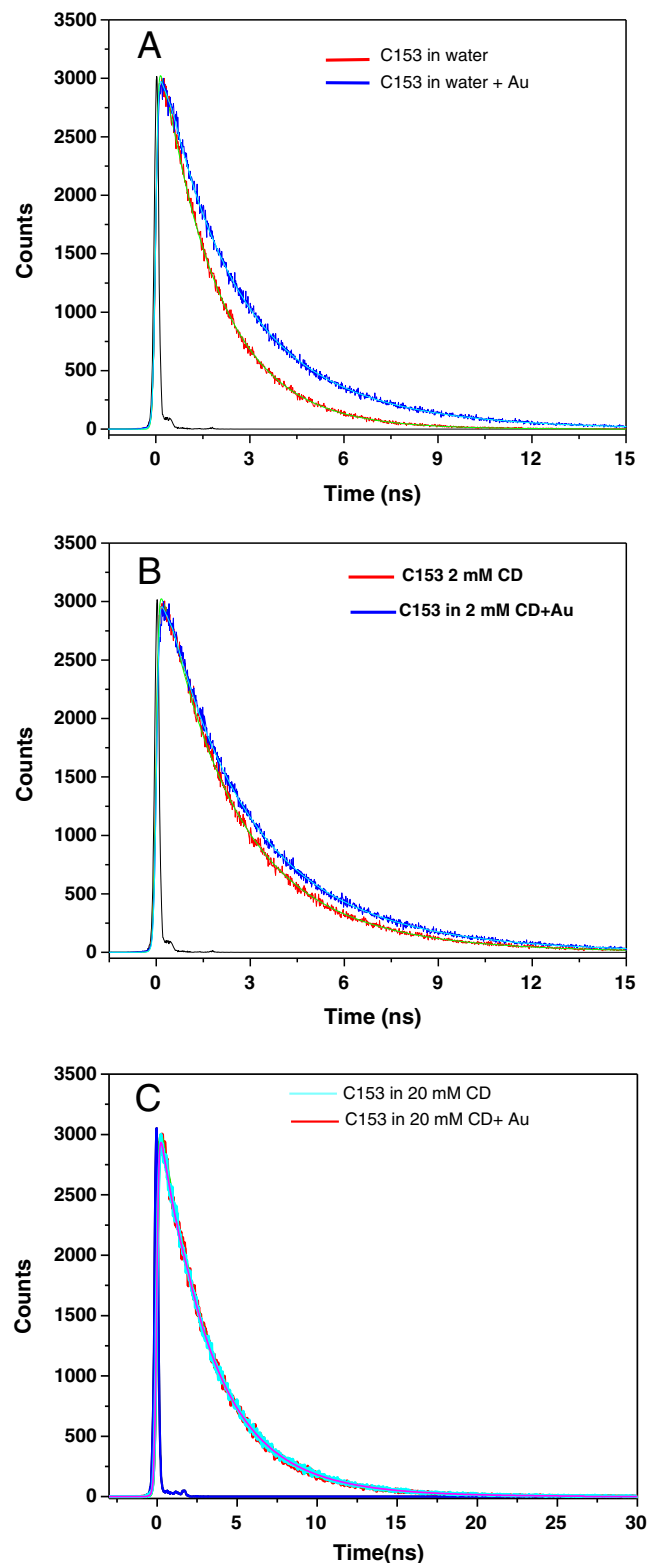


**Fig. 4** Decay curves of C153 dye in presence and absence of 1 nM Au nanoparticles; in water (a), in 2 mM  $\gamma$ -CD (b) and in 20 mM  $\gamma$ -CD concentration (c). ( $\lambda_{ex}=405$  nm)

**Table 1** Fluorescence decay parameters of C153 dye in absence and presence of Au nanoparticles and  $\gamma$ -CD ( $\lambda_{em}=536$  nm)

Systems	$\tau_1$ ( $a_1$ ) (ns)	$\tau_2$ ( $a_2$ ) (ns)	$\langle\tau\rangle$ (ns)
Pure C153	1.79 (1)	–	1.79
Pure C153+Au	1.72 (0.49)	3.35 (0.51)	2.55
C153+2 mM CD	1.91 (0.65)	3.45 (0.35)	2.45
C153 +2 mM CD+Au	1.95 (0.45)	3.58 (0.55)	2.85
C153+20 mM CD	1.78 (0.29)	3.71 (0.71)	3.15
C153+20 mM CD+Au	1.84 (0.33)	3.87 (0.67)	3.20

saturated at 2 nM Au concentration. Therefore, all the free C153 dye in water became aggregated above this Au nanoparticles concentration. H-aggregation of C153 is further confirmed by analyzing Fig. 3. Figure 3 depicts the normalized emission spectra of C153 confined in 2 mM CD in presence of 1 nM Au nanoparticles concentration. In this case we have excited the sample by two different excitation wavelengths (405 nm and 350 nm). Both peaks at 470 nm and 540 nm are prominent during 405 nm excitation where the peak at 470 nm is due to H-aggregation. The blue shifted absorption peak at 350 nm as seen from absorption spectra is considered for H-aggregation. To confirm this, further we have excited C153 in presence of 1 nM Au (confined in 2 mM CD) at 350 nm wavelength of excitation. As we excite C153 at 350 nm in presence of Au nanoparticles, only H-aggregated moieties will be excited. Interestingly, the emission band at 470 nm without the emission band at 540 nm further confirms the formation of H-aggregation in presence of Au nanoparticles. Analysis suggests that the H-aggregation of

C153 dye is found in presence of Au nanoparticles and the H-aggregation of dye molecules can be avoided in presence of  $\gamma$ -CD due to confinement of dye in nanocavity.

**Time Resolved Spectroscopic Study**

The effects of  $\gamma$ -CD and Au nanoparticles on the H-aggregation of C153 dye are again properly supported by decay time data obtained from time-resolved spectroscopy. The decay time of free C153 in water is 1.79 ns. In presence of 2 nM Au nanoparticles, fast component is 1.72 ns (49%) and slow component is 3.35 ns (51%) and the average life time is 2.55 ns (Fig. 4a). Fast component is due to free dye and slow component is due to aggregation

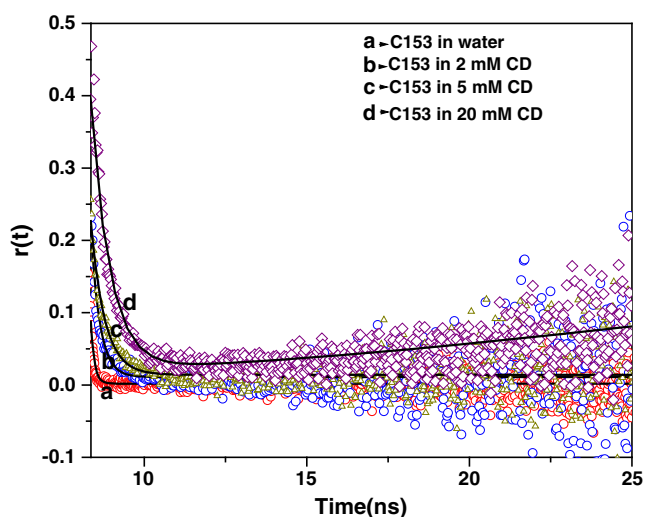


**Fig. 5** Anisotropic decay curves of C153 in water (a), confined in 2 mM  $\gamma$ -CD (b), 5 mM  $\gamma$ -CD (c) and 20 mM  $\gamma$ -CD (d). ( $\lambda_{ex}=405$  nm)

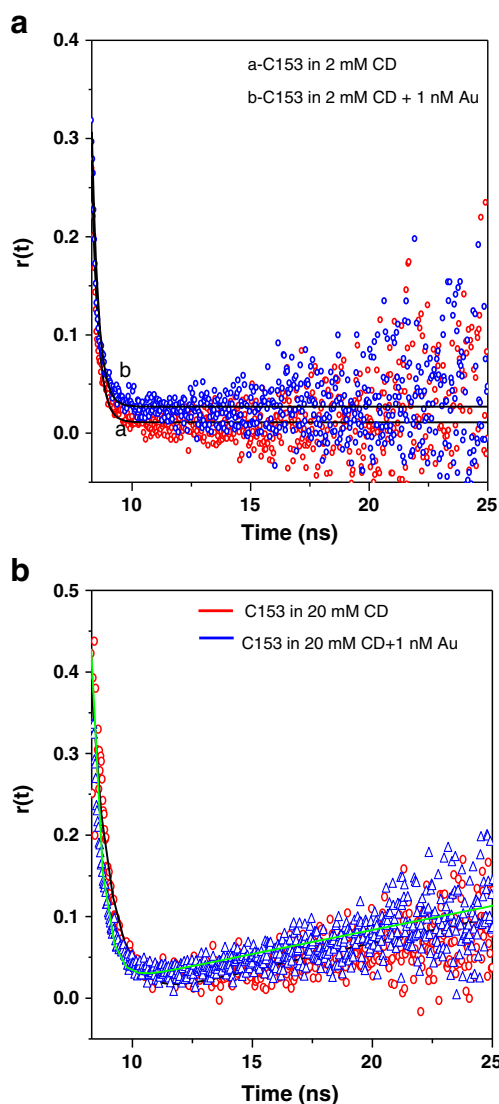


**Fig. 6** Anisotropic decay curves of C153 in absence and presence of 1 nM Au nanoparticles confined in (a) 2 mM and (b) 20 mM  $\gamma$ -CD concentration. ( $\lambda_{ex}=405$  nm)

**Table 2** Normal anisotropy decay parameters of C153 dye in different systems

Systems	$r_0$	$\alpha_1$	$\alpha_2$	$\tau_1$ (ns)	$\tau_2$ (ns)	$\langle\tau\rangle$ (ns)
C153 in water	0.15	1	–	0.11	–	0.11
C153 in water+Au	0.22	1	–	0.13	–	0.13
C153 in 2 mM $\gamma$ -CD	0.24	1	–	0.27	–	0.27
C153 in 2 mM CD+Au	0.3	0.6	0.4	0.27	0.34	0.3
C153 in 5 mM CD	0.27	1	–	0.42	–	0.42

of dye. In case of 2 mM  $\gamma$ -CD confined systems, the decay time of C153 is 2.45 ns and this decay time is increased to 2.85 ns in presence of Au nanoparticles (Fig. 4b). It is known that the decay time in aggregated state is always higher due to dipole forbidden by momentum selection rule [38]. Figure 4c shows the decay curves of C153 confined in 20 mM CD with out and in presence of 1 nM Au nanoparticles. Here, there is almost no change of average decay time in presence of Au nanoparticles in this time scale. The increment of decay time value is 6.6%, 2.3% and 1.6% for 5 mM, 10 mM and 20 mM  $\gamma$ -CD concentration, respectively. Blue shifting of PL band and the enhancement of decay time of C153 dye confirm the formation of H-aggregation. All decay data are given in Table 1. In our view, ultra fast spectroscopic study is essential for deeper understanding of this phenomenon.

### Fluorescence Anisotropy Decay Study

Fluorescence anisotropy decay study reveals the re-orientation dynamics of the excited fluorophore which directly help to understand structural information. Many groups reported earlier that the anisotropy decay of dye molecules is slower inside CD cavity compared to that in bulk water [30–33]. We have also studied the time-resolved anisotropy to understand the rotational dynamics of C153 confined in different amount of  $\gamma$ -CD. Figure 5 shows the anisotropy decay of C153 free in water and confined in 2 mM, 5 mM and 20 mM CD concentration. It is seen from Fig. 6a that a little increase in anisotropy is obtained in presence of Au nanoparticles (Table 2) in 2 mM  $\gamma$ -CD concentration. It is important to note that system became more anisotropic with increasing the CD concentration. An anomalous behavior of anisotropic decay is found in case of C153 at 20 mM  $\gamma$ -CD both in

absence and presence of Au nanoparticles (Fig. 6b). It shows a minima at short time and increases at long times. This type of decay is known as associated anisotropy decay [33] which is generally observed in biological systems. It may be due to formation of nanotubular aggregation of CD [39, 40]. The formation of the  $\gamma$ -CD aggregated nanotubular structures is based on the contribution of two forces. One is the van der Waals force of attraction between C153 and the interior of the CD cavity; the other is the H-bonding interaction between the ring OH groups of the cyclodextrin moieties, which result the self-association of  $\gamma$ -CDs.

The rotational diffusion of molecules in a homogeneous environment can be described by the model of general ellipsoids [41, 42]. The anisotropy decay  $r(t)$  can be analyzed using the equation

$$r(t) = r_0 \sum_i \exp(-t/\phi_i) \quad i = 1, 2, \dots \quad (2)$$

where  $r_0$  is the fundamental anisotropy at the time  $t=0$ , and  $\phi_i$  are the rotational correlation times for rotations around the different rotational axes of the molecule. Here, the fluorescence decay time  $\tau_i$  does not influence the anisotropy decay. The rotational relaxation time of free C153 is 0.113 ns and the  $r_0$  value is 0.154 for free C153 in water. The average relaxation time for 2 mM and 5 mM  $\gamma$ -CD systems are 0.275 ns and 0.425 ns respectively. All these data are shown in Table 2. However, the anisotropy decay of a heterogeneous environment (Fig. 5d) cannot be described by the above simple exponential approach. The anisotropy from the mixture is an intensity weighting average of the contribution from the probe in environment [41]

$$r(t) = r_1(t)f_1(t) + r_2(t)f_2(t) \quad (3)$$

**Table 3** Anisotropic decay parameters of C153 dye in 20 mM  $\gamma$ -CD

Systems	$r_0$	$\alpha_1$	$\alpha_2$	$\tau_1$ (ns)	$\tau_2$ (ns)	$\phi_1$ (ns)	$\phi_2$ (ns)
C153 in 20 mM $\gamma$ -CD	0.4	0.31	0.69	2.29	3.7	0.59	33
C153 in 20 mM $\gamma$ -CD+Au	0.42	0.37	0.63	2.39	3.85	0.43	50

Where  $r_1(t)$  and  $r_2(t)$  are the anisotropy decays in each environment and  $f_i$  are the fractional contributions of the decays in each environment. For single exponential decay, the fractional contribution is given by

$$f_i(t) = \frac{\alpha_i \exp\left(-\frac{t}{\tau_i}\right)}{\alpha_1 \exp\left(-\frac{t}{\tau_1}\right) + \alpha_2 \exp\left(-\frac{t}{\tau_2}\right)} \quad (4)$$

Thus, by using Eq. 4, the Eq. 3 can be rewritten as

$$r(t) = r_1(t) \frac{\alpha_1 \exp\left(-\frac{t}{\tau_1}\right)}{\alpha_1 \exp\left(-\frac{t}{\tau_1}\right) + \alpha_2 \exp\left(-\frac{t}{\tau_2}\right)} + r_2(t) \times \frac{\alpha_2 \exp\left(-\frac{t}{\tau_2}\right)}{\alpha_1 \exp\left(-\frac{t}{\tau_1}\right) + \alpha_2 \exp\left(-\frac{t}{\tau_2}\right)} \quad (5)$$

Now, by using Eqs. 2, 5 can be rearranged as

$$r(t) = \frac{\sum_i \alpha_i \exp\left(-\frac{t}{\tau_i}\right) r_{0i} \exp\left(-\frac{t}{\phi_i}\right)}{\sum_i \alpha_i \exp\left(-\frac{t}{\tau_i}\right)} \quad i = 1, 2, \dots \quad (6)$$

Here,  $\alpha_i$  is the pre-exponential factors of the anisotropy decay. In such systems it is assumed that each fluorescence decay time  $\tau_i$  is directly associated with one rotational correlation time  $\phi_i$ , the observed anisotropy decay  $r(t)$  in the case of two microenvironments results in a complex decay. The value  $r_{0i}$  is kept constant, because no alteration in the fundamental anisotropy  $r_0$  of the dyes due to binding is expected. Using a global fitting approach, the fluorescence anisotropy decay curve of C153 in 20 mM  $\gamma$ -CD (Fig. 6a) is fitted by using Eq. 6, with the fluorescence decay times  $\tau_1$  and  $\tau_2$ , as well as the rotation correlation times  $\phi_1$  and  $\phi_2$  set as global parameters. The fitted results are enlisted in Table 3. The fluorescence decay times are 2.29 ns and 3.7 ns; and the rotational correlation times are 598 ps and 33 ns. The decay time of 2.29 ns and fast correlation time of 598 ps is due to unbound free dye (31%) present in water and the decay time of 3.7 ns and large correlation time of 33 ns originates from the rotation of the  $\gamma$ -CD bound dye molecules (69%), whose rotational volume is very high due to the formation of the nanotubular structures. The anisotropy decay of C153 confined in 20 mM  $\gamma$ -CD in presence of Au nanoparticles also shows anomalous anisotropic behavior and the anisotropy decay was fitted by using Eq. 6. The fitted results are enlisted in Table 3. The fluorescence decay times are 2.39 ns and 3.85 ns; and the rotational correlation times are 430 ps and 50 ns. In this circumstance, there is no effective interaction of C153 molecules with Au nanoparticles. This observation correlates with the previous data obtained from steady state

photoluminescence spectra and time resolved decay time measurements.

## Conclusion

In conclusion, we report the formation of H-aggregation of C153 dye molecules in presence of Au nanoparticles and the influence of  $\gamma$ -cyclodextrin on the dye aggregation. Blue shifting of absorption and PL band and the enhancement of decay time of C153 dye confirm the formation of H-aggregation. The anisotropy decay reveals that the dye molecules are confined inside  $\gamma$ -cyclodextrin channels. An associated type anisotropy decay of C153 dye is found in high concentration of CD which is explained due to formation of nanotubular aggregates of  $\gamma$ -CD. Such system could pave the way for designing new optical based materials for the application in chemical sensing or light harvesting system.

**Acknowledgement** A.P thanks to DST, CSIR and “Ramanujan Fellowship” for generous funding. SB, TS and SM thank CSIR for awarding fellowship

## References

- Persson BN, Lang ND (1982) Electron-hole-pair quenching of excited states near a metal. *Phys Rev B* 26:5409–5415
- Alivisatos AP, Waldeck DH, Harris CB (1985) Nonclassical behavior of energy transfer from molecule to metal surfaces: biacetyl( $^3n\pi^*$ )/Ag(111). *J Chem Phys* 82:541–547
- Dulkeith E, Morteaux AC, Niedereichholz T, Khar TA, Feldmann J, Levi SA, Veggel FCJM, Reinhoudt DN, Moller M, Gittins DI (2002) Fluorescence quenching of dye molecules near gold nanoparticles: radiative and nonradiative effects. *Phys Rev Lett* 89, 203002:1–4
- Yun CS, Javier A, Jennings T, Fisher M, Hira S, Peterson S, Hopkins B, Reich NO, Strouse GF (2005) Nanometal surface energy transfer in optical rulers, breaking the FRET barrier. *J Am Chem Soc* 127:3115–3119
- Sen T, Sadhu S, Patra A (2007) Surface energy transfer from rhodamine 6 G to gold nanoparticles: a spectroscopic ruler. *Appl Phys Lett* 91:043104-1-3
- Sen T, Patra A (2008) Resonance energy transfer from rhodamine 6 G to gold nanoparticles by steady-state and time-resolved spectroscopy. *J Phys Chem C* 112:3216–3222
- Sen T, Patra A (2009) Formation of self-assembled Au nanoparticles and the study of their optical properties by steady-state and time-resolved spectroscopies. *J Phys Chem C* 113:13125–13132
- Haldar KK, Sen T, Patra A (2008) Au@ZnO core-shell nanoparticles are efficient energy acceptors with organic dye donors. *J Phys Chem C* 112:11650–11656
- Nasar CP, Liu D, Hotchandani S, Kamat PV (1996) Dye-capped semiconductor nanoclusters. Excited state and photosensitization aspects of rhodamine 6 G H-aggregates bound to SiO<sub>2</sub> and SnO<sub>2</sub> colloids. *J Phys Chem* 100:11054–11061
- Xu P, Yangi H (1999) Fluorescence patterning in dye-doped sol-gel films by generation of gold nanoparticles. *Chem Mater* 11:2626–2628

11. Khan SS, Jin ES, Sojic N, Pantano PA (2000) Fluorescence-based imaging-fiber electrode chemical sensor for hydrogen peroxide. *Anal Chim Acta* 404:213–221
12. Ganapathy S, Sengupta S, Wawrzyniak PK, Huber V, Buda F, Baumeister U, Wurthner F, Groot HJMD (2009) Zinc chlorins for artificial light-harvesting self-assemble into antiparallel stacks forming a microcrystalline solid-state material. *PNAS* 106:11472–11477
13. Kim S, Ohulchanskyy TY, Pudavar HE, Pandey RK, Prasad PN (2007) Organically modified silica nanoparticles co-encapsulating photosensitizing drug and aggregation-enhanced two-photon absorbing fluorescent dye aggregates for two-photon photodynamic therapy. *J Am Chem Soc* 129:2669–2675
14. Das S, Kamat PV (1999) Can H-aggregates serve as light-harvesting antennae? Triplet–triplet energy transfer between excited aggregates and monomer thionine in aerosol-OT solutions. *J Phys Chem B* 103:209–215
15. Khazraji AC, Hotchandani S, Das S, Kamat PV (1999) Controlling dye (Merocyanine-540) aggregation on nanostructured TiO<sub>2</sub> films. An organized assembly approach for enhancing the efficiency of photosensitization. *J Phys Chem B* 103:4693–4700
16. Chaudhuri D, Li D, Che Y, Shafran E, Gerton JM, Zang L, Lupton JM (2011) Enhancing long-range exciton guiding in molecular nanowires by H-aggregation lifetime engineering. *Nano Lett* 11:488–492
17. Chandrasekharan N, Hu J, Jones G II, Kamat PV (2000) Dye-capped gold nanoclusters: photoinduced morphological changes in gold/rhodamine 6 G nanoassemblies. *J Phys Chem B* 104:11103–11109
18. Kerker M (1985) The optics of colloidal silver: something old and something new. *J Colloid Interface Sci* 105:297–314
19. Ghosh SK, Pal A, Nath S, Kundu S, Panigrahi S, Pal T (2005) Dimerization of eosin on nanostructured gold surfaces: size regime dependence of the small metallic particles. *Chem Phys Lett* 412:5–11
20. Hranisavljevic J, Dimitrijevic NM, Wurtz GA, Wiederrecht GP (2002) Photoinduced charge separation reactions of J-aggregates coated on silver nanoparticles. *J Am Chem Soc* 124:4536–4537
21. Kometani N, Tsuboishi M, Fujita T, Asani K, Yonezawa Y (2001) Preparation and optical absorption spectra of dye-coated Au, Ag, and Au/Ag colloidal nanoparticles in aqueous solutions and in alternate assemblies. *Langmuir* 17:578–580
22. Su GJ, Yin SX, Wan LJ, Zhao JC, Bai CL (2003) A dimeric structure of eosin molecules on Au(1 1 1) surface. *Chem Phys Lett* 370:268–273
23. Uwada T, Toyota R, Masuhara H, Asahi T (2007) Single particle spectroscopic investigation on localized surface plasmon resonance of gold nanoparticles coated with cyanine dye J-aggregates. *J Phys Chem* 111:1549–1552
24. Calzaferri G, Huber S, Maas H, Minkowski C (2003) Host–guest antenna materials. *Angew Chem Int Ed* 42:3732–3758
25. Nguyen TQ, Wu J, Doan V, Schwartz BJ, Tolbert SH (2000) Control of energy transfer in oriented conjugated polymer-mesoporous silica composites. *Science* 288:652–656
26. Borja M, Dutta PK Storage of light energy by photoelectron transfer across a sensitized zeolite-solution interface. *Nature* 362:43–45
27. Hernandez R, Franville AC, Minoofar P, Dunn B, Zink JI (2001) Controlled placement of luminescent molecules and polymers in mesostructured sol-gel thin films. *J Am Chem Soc* 123:1248–1249
28. Sen T, Jana S, Koner S, Patra A (2010) Energy transfer between confined dye and surface attached au nanoparticles of mesoporous silica. *J Phys Chem C* 114:707–714
29. Szteli J (1998) Introduction and general overview of cyclodextrin chemistry. *Chem Rev* 98:1743–1753
30. Li G, McGown LB (1994) Molecular nanotube aggregates of  $\beta$ - and  $\gamma$ -cyclodextrins linked by diphenylhexatrienes. *Science* 264:249–251
31. Harada A, Li J, Kamachi M (1992) The molecular necklace: a rotaxane containing many threaded  $\alpha$ -cyclodextrins. *Nature* 356:325–327
32. Harada A, Li J, Kamachi M (1993) Synthesis of a tubular polymer from threaded cyclodextrins. *Nature* 364:516–518
33. Roy D, Mondal SK, Sahu K, Ghosh S, Sen P, Bhattacharyya K (2005) Temperature dependence of anisotropy decay and solvation dynamics of coumarin 153 in  $\gamma$ -cyclodextrin aggregates. *J Phys Chem A* 109:7359–7364
34. Sen T, Haldar KK, Patra A (2010) Quenching of confined C480 dye in the presence of metal-conjugated  $\gamma$ -cyclodextrin. *J Phys Chem C* 114:11409–11413
35. Grabar KC, Freeman RG, Hommer MB, Natan MJ (1995) Preparations and characterization of Au colloid monolayers. *Anal Chem* 67:735–743
36. Sen T, Jana S, Koner S, Patra A (2010) Efficient energy transfer between confined dye and Y-zeolite functionalized Au nanoparticles. *J Phys Chem C* 114:19667–19672
37. Ghosh S, Mondal SK, Sahu K, Bhattacharyya K (2006) Ultrafast electron transfer in a nanocavity. Dimethylaniline to coumarin dyes in hydroxypropyl  $\gamma$ -cyclodextrin. *J Phys Chem A* 110:13139–13144
38. Meinardi F, Cerminara M, Sassella A, Bonifacio R, Tubino R (2003) Superradiance in molecular H aggregates. *Phys Rev Lett* 91:247401
39. Jaffer SS, Saha SK, Eranna G, Sharma AK, Purkayastha P (2008) Intramolecular charge transfer probe induced formation of  $\alpha$ -cyclodextrin nanotubular suprastructures: a concentration dependent process. *J Phys Chem C* 112:11199–11204
40. Jaffer SS, Saha SK, Purkayastha P (2009) Fragmentation of molecule-induced  $\gamma$ -cyclodextrin nanotubular suprastructures due to drug dosage. *J Colloids Interface Sci* 337:294–299
41. Lakowicz JR (2006) Principles of fluorescence spectroscopy, 3rd edn. Springer, New York
42. Lushtinetz F, Dosche C, Kumke MU (2009) Influence of streptavidin on the absorption and fluorescence properties of cyanine dyes. *Bioconjugate Chem* 20:576–582